

Study on Enzymatic and Electrochemical Properties of Cellulase Immobilized with Multi-Walled Carbon Nanotubes as Sensor for Catechol

Junling Wang¹, Jingnan Wang¹, Wenxu Li², Chuang Yang^{2,*}

¹College of Biological and Pharmaceutical Engineering, Jilin Agricultural Science and Technology University, Jilin 132101, China

²College of Agriculture, Jilin Agricultural Science and Technology University, Jilin 132101, China

*E-mail: yc2996251@sina.com and yangchuang@jlnku.edu.cn

Received: 3 January 2021 / Accepted: 22 February 2021 / Published: 28 February 2021

This work focused on studying the enzymatic and electrochemical properties of cellulase immobilized on carboxylated MWCNTs (cellulase/c-MWCNTs). The morphology and attachment of impurities, enzymatic and electrochemical properties of c-MWCNTs and cellulase/c-MWCNTs were studied. Results of morphology and attachment of impurities by FESEM and FTIR showed that the c-MWCNTs were prepared in bundles structure with porous and smooth surface but after cellulase immobilization by entrapment inside c-MWCNTs matrix, the prepared cellulase/c-MWCNTs displayed the rougher surface with more saturated pores. These results of FTIR evidenced to form N–H and O–H stretching vibrations of cellulase, and presence of nitriles, amide group and aliphatic amide bond in cellulase/c-MWCNTs structure that confirmed to successfully immobilization of cellulase enzyme on the c-MWCNTs side walls. Study of enzymatic properties showed that the optimum condition for electrochemical study of the cellulase/c-MWCNTs was concentration of 4 mg/ml, pH 4 and temperature of 35°C. Electrochemical study of cellulase/c-MWCNTs for detection catechol showed linear range and detection limit were obtained 10 to 160 µM and 0.004 µM, respectively. The comparison of sensing properties of cellulase/c-MWCNTs and other reported catechol sensors indicated the comparable electrochemical properties. Low detection limit for determination of catechol on the cellulase/c-MWCNTs can be due to formation of fast electron transfer pathways between the cellulase/c-MWCNTs electrode and the electrolyte.

Keywords: Enzymatic property; Electrochemical sensor; Cellulase; Carbon nanotubes; Cyclic voltammetry; Amperometry

1. INTRODUCTION

Cellulase (C₁₈H₃₂O₁₆) as multi-enzyme system is synthesized from several microorganisms such as fungal species (*Lichtheimia romosa*, *Dipodascaceae*, *Phaffomycetaceae*, *Humicola insolens* and

Trichoderma citrinoviride), bacterial species (Bacillus, Trichoderma reesei, Paenibacillus chitinolyticus CKS1, Clostridium thermocellum and Ochrobactrumsp K38), actinomycetes and protozoans [1, 2]. In addition, Cellulase can be produced in agricultural and forestry residues, aquatic plants, organic components of municipal solid waste, woody and herbaceous biomass. This enzyme includes several kinds of enzymes such as β -1,4-endoglucanases, β -glucosidase, β -1,4-exoglucanases (cellobiohydrolases), β -xylosidase, and β -1,4-glucosidases [1].

This enzyme also completely hydrolysis polysaccharide carbohydrates like cellulose, starch, glycogen and chitin. On the other hand, it can break down cellulose molecules to glucose. Cellulase is widely used in food and pharmaceutical processing, animal feed production, fermentation of biomass into biofuels, composting, laundry detergents, agriculture, textile wet processing, detergent, pulp, and paper bleaching.

Meanwhile, use of free molecules of cellulase shows some problems for separation, recovery of used molecules and their repeatability and reusability after hydrolysis reaction [3, 4]. By considering the high price of the enzyme, enzyme immobilization is a beneficial method that enhances the enzyme repeatability and reusability [5-9]. Both physical and chemical adsorptions are the immobilization methods which lead to formation of hydrophobic, covalent and hydrogen bindings between the enzyme molecules and substrates [10-13]. Studies showed that entrapment of biomolecules in sol-gel, silica, polymers, composites, graphene, MWCNTs and nanostructured matrixs not only have been improved the enzymatic activity and stability but also it is cost effective [14-19]. For example, Zhang et al. [20] synthesized functionalized magnetic Fe_3O_4 nanospheres with core-shell morphologies and used for cellulase immobilization. Their results showed that cellulase immobilization capacity has been enhanced with increasing surface charge of nanospheres. Zhang et al. [21] immobilized cellulase onto silica gel surfaces and showed the activity of the immobilized cellulase was enhanced 7 ± 2 % compared to the free cellulase sample. Thus, this study focused on investigation of the enzymatic and electrochemical properties of cellulase immobilized on carboxylated MWCNTs.

2. EXPERIMENT

In order to immobilize the enzyme on MWCNTs, 50 mg of MWCNTs (< 80%, outer diameter of 20-40 nm, length of 10-30 μm , XingtaiShineway Corporation Co., Ltd., China) was added to 200 ml of mixture of nitric acid (68%, Qingdao HiseaChem Co., Ltd., China) and sulphuric acid (98%, Qingdao HiseaChem Co., Ltd., China) at a volume ratio of 1:2 (v:v). The resulting mixture was dispersed in an ultrasonic bath at 35 $^{\circ}\text{C}$ for 5 hours to combine the acid mixture and functionalize the MWCNTs surface. The c-MWCNTs was washed with deionized water and filtered with hydrophilized PTFE membrane (0.2 - 0.65 μm , JiAn City Qingfeng Filter Equipment Material Co., Ltd., China). Then, acid cellulase enzyme (Zibo Aoqiang Chemical Co., Ltd., China) was added to 50 mL food buffer sodium phosphate monobasic (50 mM, 98%, Shanghai Sky Chem Industrial Co., Ltd., China), 5 ml citric acid (99.5%, Hunan MingruiXiangsheng Trade Co., Ltd., China) and c-MWCNTs. The suspension was ultrasonically stirred for 2 hours. Then, 200 mL of 4 % sodium alginate (Qingdao Yingfei Chemical Co., Ltd., China) was added to the stirred suspension. After then, the cellulase

immobilized with MWCNTs (cellulase /MWCNT) suspension was centrifuged at 2500 rpm for 10 minutes, followed by washing and immersion in fresh phosphate buffer solution (PBS) to remove any unbound enzyme and immersion. Finally, cellulase /MWCNT was dropped on GCE and left to air dry for 12 hours and stored for further characterization.

Field emission scanning electron microscopy (FESEM S-4800, Hitachi, Tokyo, Japan) analysis was used to study the structural and surface morphologies of the c-MWCNTs and cellulase/c-MWCNTs. Fourier transform infrared (FTIR, Xi'an Heb Biotechnology Co., Ltd., China) spectroscopy analysis was conducted in the range 500 to 4000 cm^{-1} to study the attachment of impurities on MWCNTs.

In order to study of enzyme activity, the mixture of 2 ml of 0.1 M PBS, 1 ml of carboxymethylcellulose (90%, Linyi Jindi Chemical Co., Ltd., China) and 1 ml (U/mL) of acid cellulase enzyme was prepared. Then, 6 ml of 3, 5-dinitrosalicylic acid (Seebio Biotech (Shanghai) Co., Ltd., China) was added in an ultrasonic bath at 95 °C for 20 minutes. After cooling, 10 ml of de-ionized water was added to the obtained mixture. The absorbance of 3, 5-dinitrosalicylic acid was measured at 540 nm using the UV-vis spectrophotometer (Bench Top N6000, Shanghai Yoke Instrument Co., Ltd., China). 1 ml de-ionized water as the blank control was serially added to the enzyme solution. Hydrolysis of cellulase formed 3- amino-5-nitrosalicylic acid which showed the maximum absorbance at 540 nm [22]. Therefore, optical density was proportional to the reduction of cellulase or enzyme activity [23]. The immobilized enzyme activity obtained by equation (1) where t and g are the reaction time and amount of immobilized enzyme on MWCNTs [23, 24]:

$$\text{Enzyme activity} = \frac{\text{reduction of cellulase (mg)}}{0.18 \text{ tg}} \quad (1)$$

Cyclic voltammetry (CV) and amperometry for electrochemical characterization of prepared samples were performed with potentiostat (Autolab PGSTAT 302N, EcoChimie B.V.) in standard three-electrode electrochemical cell using prepared electrode as the working electrodes, a platinum foil as the counter electrode and an Ag/AgCl (KCl, 3 M) as reference electrode. 0.1 M phosphate buffer solutions (PBS) was used as electrolyte in electrochemical cell which prepared from 0.1 M H_3PO_4 ($\geq 85\%$, Hebei Mojin Biotechnology Co., Ltd., China) and 0.1 M NaH_2PO_4 (98%, Hebei Mojin Biotechnology Co., Ltd., China). The pH of solutions was adjusted by HCl (36%, Qingdao HiseaChem Co., Ltd., China) and NaOH (99%, ZoupingBoyi Chemical Industry Co., Ltd., China).

In order to determine the catechol in real samples, the commercially available green tea sample of Lipton brand was purchased from a supermarket and crushed to powder using a mortar, and then 0.1 g of dry powder was mixed to 100 ml of 0.1 M PBS pH 4.0. The mixture was shaken for 15 minutes at 90 °C, and filtered and diluted to 100 ml of 0.1 M PBS pH 4.0 containing 5 mM $[\text{Fe}(\text{CN})_6]^{3-/4-}$, and stored for further studies.

3. RESULTS AND DISCUSSION

FESEM images of c-MWCNTs and cellulase/c-MWCNTs are presented in Figure 1. As observed, there are c-MWCNTs bundles with porous and smooth surface with length in the range of 4

μm to $6\ \mu\text{m}$ and diameter in the range of $40\ \text{nm}$ to $70\ \text{nm}$. After cellulase immobilization, the FESEM image of cellulase/c-MWCNTs shows the rougher surface with more saturated pores which indicated the porous and smooth surfaces of c-MWCNTs are appropriate sites for absorption of enzyme and successfully immobilization of cellulase enzyme molecules on c-MWCNTs surface. It suggested that there are relatively high numbers of hydrophobic amino acids on cellulase surfaces which can form covalent bonds with hydroxyl and carboxylic groups on c-MWCNTs bundles [25].

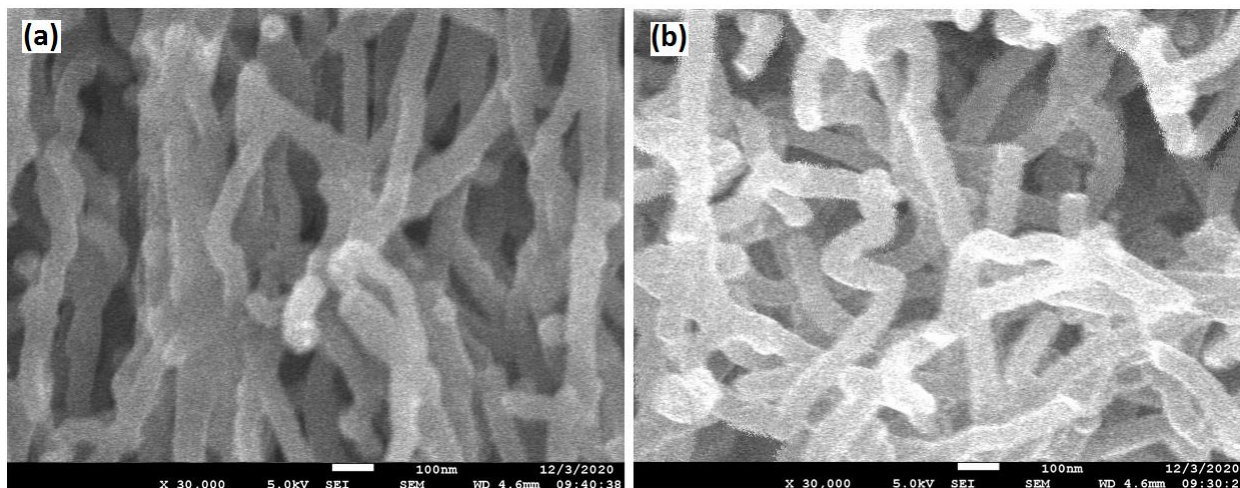


Figure 1. FESEM images of (a) c-MWCNTs and (b) cellulase/c-MWCNTs.

FTIR spectrums of MWCNTs, c-MWCNTs and cellulase/c-MWCNTs are shown in Figure 2. For MWCNTs sample (Figure 2a), FTIR spectrum shows the peak at $1090.20\ \text{cm}^{-1}$ corresponding to stretching vibrations of C–O bond in MWCNTs. The peak at $1550.12\ \text{cm}^{-1}$ is associated with C=C stretching vibration of graphite band in MWCNTs, the peaks at $2860.02\ \text{cm}^{-1}$ and $2923.21\ \text{cm}^{-1}$ relating to C–H asymmetric and symmetric stretching vibrations in MWCNTs, respectively. The peak at $3480.33\ \text{cm}^{-1}$ is assigned to stretching vibration –OH bonds, respectively [26].

The FTIR spectrum of c-MWCNTs (Figure 2b) shows the peak at $1079.28\ \text{cm}^{-1}$ describe by the introduction of carboxylic functional groups of C–O on the carbon surfaces [27]. The peak at $1391.35\ \text{cm}^{-1}$ shows the presence of stretching mode of C=C of aromatic groups on c-MWCNTs. The peak at $1655.04\ \text{cm}^{-1}$ which demonstrated the presence of C=O stretching frequency and formation of carboxylic acid groups on the side surfaces of carboxylated MWNTs. The peak at $2920.18\ \text{cm}^{-1}$ exhibits the C–H stretching vibration created at the defect sites of acid-oxidized MWCNT surface [28]. The peak at $3503.05\ \text{cm}^{-1}$ illustrates to formation of carboxylic functional groups of O–H on the carbon surfaces [27].

The FTIR spectrum of cellulase/c-MWCNTs (Figure 2c) also displays the peaks at $3451.77\ \text{cm}^{-1}$, $3378.35\ \text{cm}^{-1}$, and $3204.05\ \text{cm}^{-1}$ that these indicate to characteristic of N–H and O–H stretching vibrations of cellulase. The peaks at $2468.25\ \text{cm}^{-1}$, $1660.11\ \text{cm}^{-1}$ and $1071.02\ \text{cm}^{-1}$ are related to presence of nitriles, amide group and aliphatic amide bond in cellulase/c-MWCNTs structure [29]. Moreover, the peak at $1385.40\ \text{cm}^{-1}$ represents maintenance of the C=C stretching aromatic mode of

MWCNT after the immobilization process. These results confirm the successful immobilization of cellulase enzyme on the c-MWCNTs side walls.

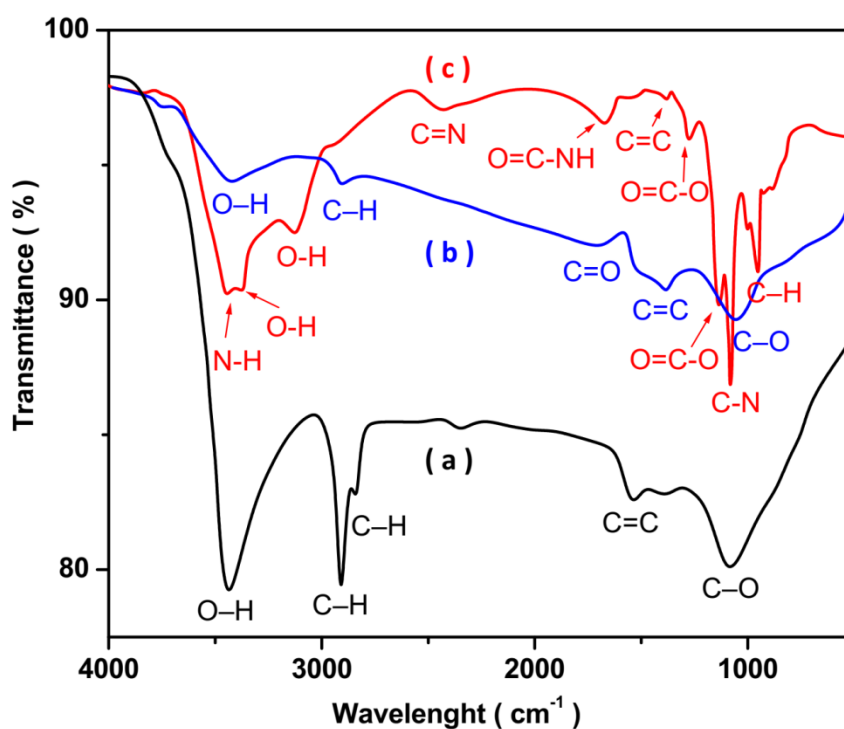


Figure 2. FTIR spectrums of (a) MWCNTs, (b) c-MWCNTs and (c) cellulase/c-MWCNTs

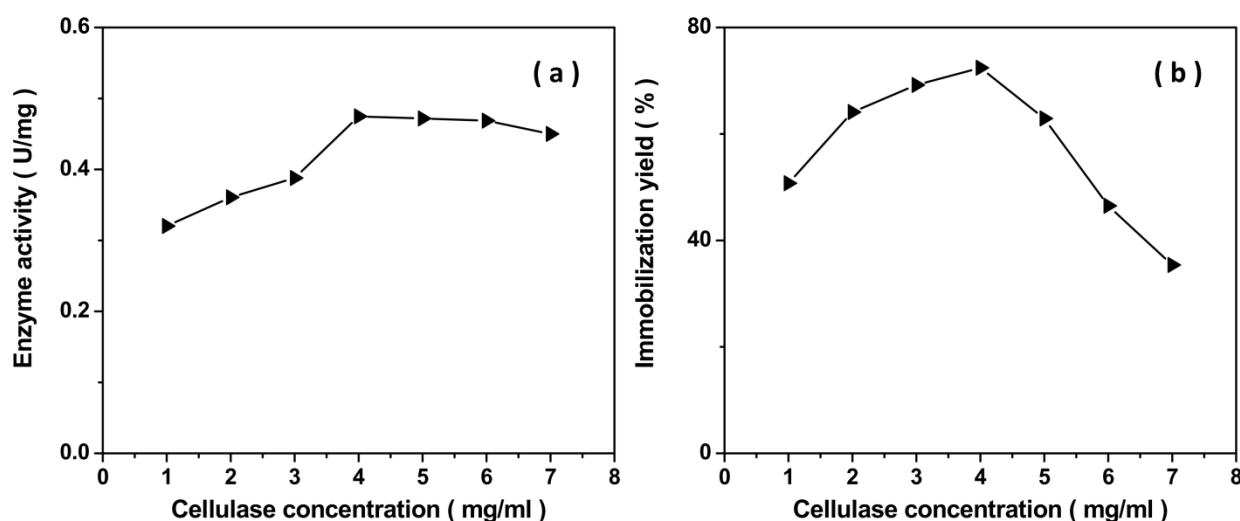


Figure 3. Influence of immobilized enzyme concentration on (a) enzyme activity and (b) immobilization yield of cellulase on MWCNTs in pH 7 at 25 °C.

In order to determine the optimum concentration of the immobilized cellulase, the influence of immobilized enzyme concentration on enzyme activity and immobilization yield of cellulase on

MWCNTs display in Figures 3a and 3b. As found from Figure 3a, the activity of immobilized enzymes is enhanced with the increasing cellulase concentration from 1 to 4 mg/ml because of large surface area and pore sites on the MWCNT side wall. In addition, the fast diffusion rates, ultimate high-strength and high ratio of carbon atoms at the edges to the carbon atoms on the basal plane of MWCNTs make them the ideal substrate for cellulase absorption [30]. For cellulase concentration more than 4 mg/ml, enzyme activity on the MWCNT is slightly decreased. Moreover, the enzyme immobilization yield variation in Figure 3b exhibits that the maximum yield is obtained at 4 mg/ml where increasing the concentration of cellulase leads to decrease immobilization yield. This decrease in immobilization yield may be related to over saturation and clustering or steric hindrance in enzyme molecules that can limit the diffusion rate [31]. The similar reports for decrease in enzyme immobilization yield with increasing enzyme concentration have been presented for lipase [32], *Bacillus licheniformis* L-arabinose isomerase [33], alcohol dehydrogenase [34], and phospholipase A1 [35]. Therefore, the 4 mg/ml is selected as optimal cellulase concentration for following measurements.

pH is another effective parameter on activity and charge transfer of enzyme. Figure 4a shows the Effect of pH on immobilized cellulase activity with concentration of 4 mg/mL at 25 °C. As observed, enzyme activity is better in acidic solutions which associated with change in electrostatic repulsions of the ionic groups on the enzyme surface with variation of pH. The highest enzyme activity is obtained at pH of 4. In both acidic and alkaline pH extreme environments, the enzyme is subjected to the unfolding force because of ionization and created electrostatic repulsion among charge groups [36]. Especially for alkaline environments, denaturation and unfolded structures of protein are generated that contain weak and unstable secondary and tertiary structures of protein [36]. The result of stability and immobilized enzyme towards change in pH is agreement with other reports of enzyme immobilization and activity [37]. Thus, the following studies are performed at pH of 4.

Further study was conducted on temperature effect on immobilized enzyme activity. Figure 4b shows the variation of enzyme activity toward the temperature and significant influence of temperature on enzyme activity. The optimum temperature for immobilized cellulase on MWCNTs is obtained 35°C. For low temperature, enzyme activity is restrained and for temperature higher than 35°C, enzyme experiences denaturation and inactivation phenomena [38]. These results indicate that the optimum condition for electrochemical study of the cellulase/c-MWCNTs is obtained concentration of 4 mg/ml, pH 4 and temperature of 35°C.

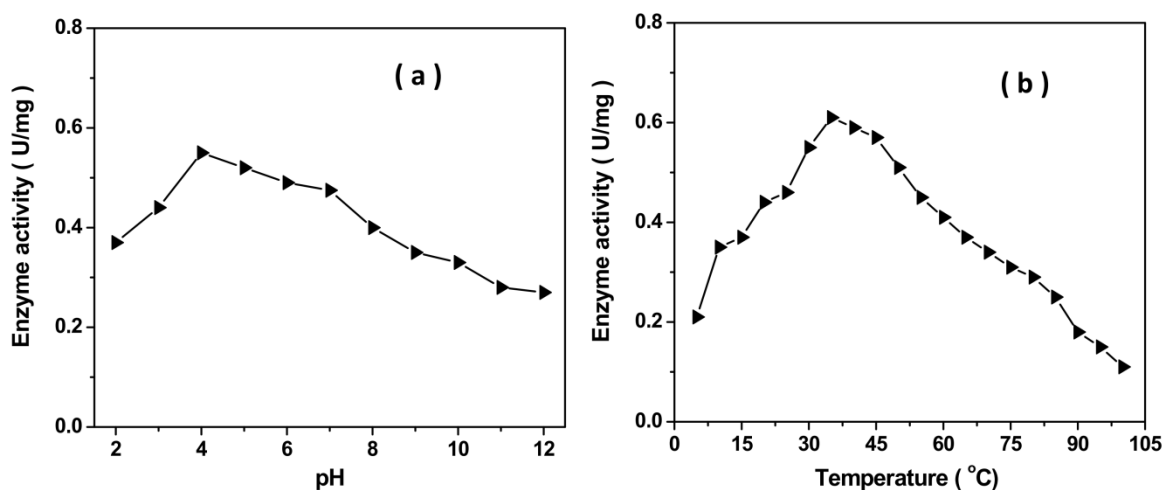


Figure 4. Influence of (a) pH (25 °C) and (b) temperature on immobilized enzyme activity (pH 4) at 4 mg/ml cellulase concentration.

The electrochemical properties of MWCNTs and cellulase/c-MWCNTs were studied through the measurement of CVs in 0.1 M PBS pH 4.0 containing 5 mM $[\text{Fe}(\text{CN})_6]^{3-/4-}$ at 50 mVs^{-1} . As seen from Figure 5, the anodic peak and cathodic peaks are at about -0.08 V and 0.11 V for both of electrodes but higher current electrochemical redox peaks are observed for cellulase/c-MWCNTs which ascribed to formation of fast electron transfer pathways between the cellulase/c-MWCNTs electrode and the electrolyte because of synergistic effect of porous morphology and nanometric cylindrical graphene sheets in the MWCNTs and crosslinking and covalent bounds of cellulase[39]. Moreover, enhancement of redox intensity on cellulase/c-MWCNTs can be related to the good biocompatibility and high surface area of MWCNTs which can provide an appropriate interface for the orientation and immobilization of cellulase molecules [40]. Therefore, cellulase/c-MWCNTs is employed for following electrochemical studies.

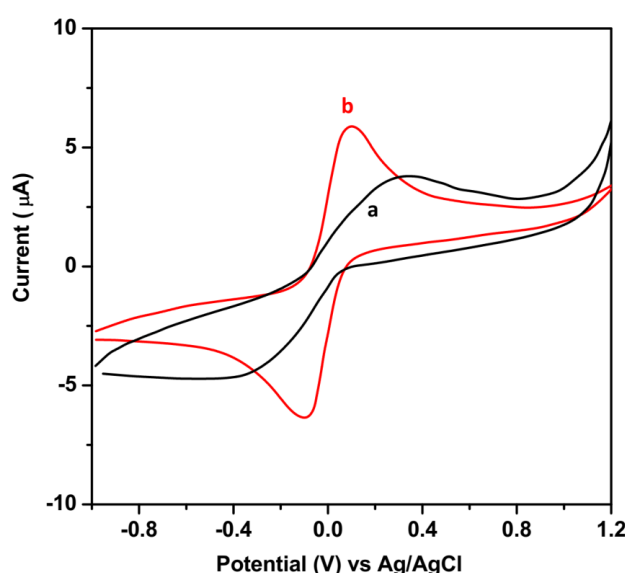


Figure 5. The recorded CVs of (a) MWCNTs and (b) cellulase/c-MWCNTs in 0.1 M PBS pH 4.0 containing 5 mM $[\text{Fe}(\text{CN})_6]^{3-/4-}$ at 50 mVs^{-1} and temperature of 35 °C.

Figure 6a shows the effect of scan rate on the electrochemical redox response of cellulase/c-MWCNTs in 0.1 M PBS pH 4.0 containing 5 mM $[\text{Fe}(\text{CN})_6]^{3-/4-}$. It can be observed that the currents of redox peaks are increased with increasing the scan rates from 10 to 100 mVs^{-1} and the potentials of redox peaks are not changed with increasing the scan rate value. Figure 6b shows the linear relationship between the peak currents and square root of scan rate values which illustrated to the diffusion controlled of electrochemical process [41].

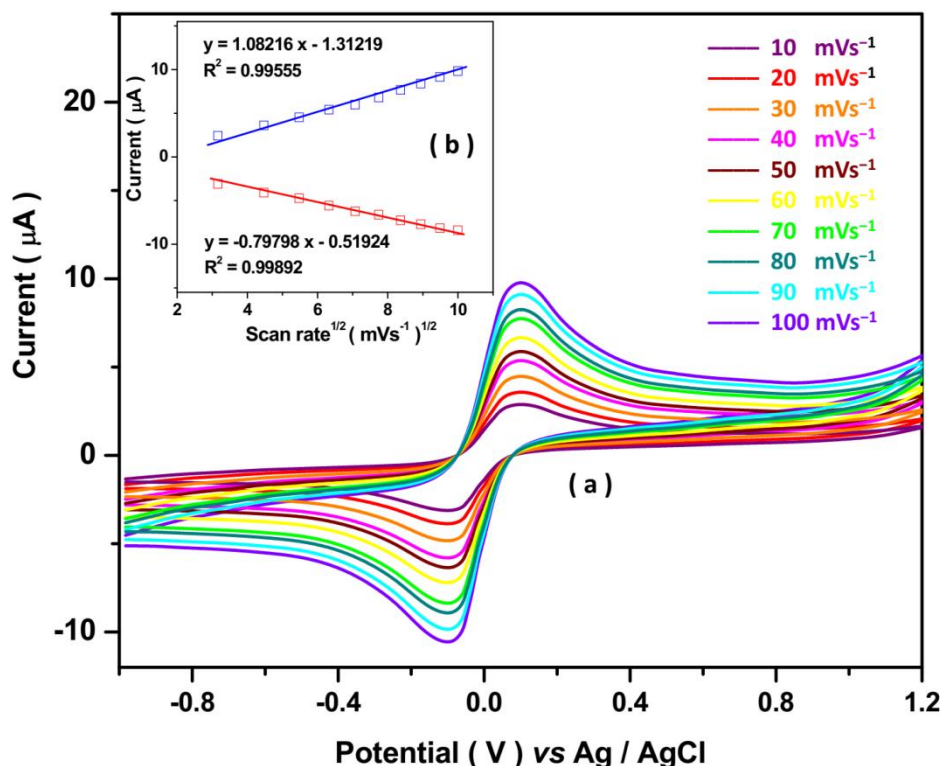


Figure 6. (a) The recorded CVs of cellulase/c-MWCNTs in 0.1 M PBS pH 4.0 containing 5 mM $[\text{Fe}(\text{CN})_6]^{3-/4-}$ at scan rates from 10 to 100 mVs^{-1} , and (b) plot of peak currents vs. square root of scan rate values and temperature of 35°C.

More electrochemical studies of cellulase/c-MWCNTs were conducted by amperometry technique for detection catechol in 0.1 M PBS pH 4.0 containing 5 mM $[\text{Fe}(\text{CN})_6]^{3-/4-}$ at potential 0.11 V. Figures 7a and 7b show the electrochemical amperometry response of cellulase/c-MWCNTs and its calibration plot for successive injection of 10 μM catechol solution which revealed the fast and linear response of electrode toward addition of catechol. The detection limit of catechol on cellulase/c-MWCNTs is obtained 0.004 μM . Furthermore, Figure 7b shows that the linear range is obtained from 10 to 160 μM for catechol determination on cellulase/c-MWCNTs. The resulted sensing properties of cellulase/c-MWCNTs are compared with other reported catechol sensor in Table 1 which specified to the comparable electrochemical properties and low detection limit for determination of catechol on the cellulase/c-MWCNTs due to porous matrix and biocompatible carboxylic acid functionalization of MWCNTs [42].

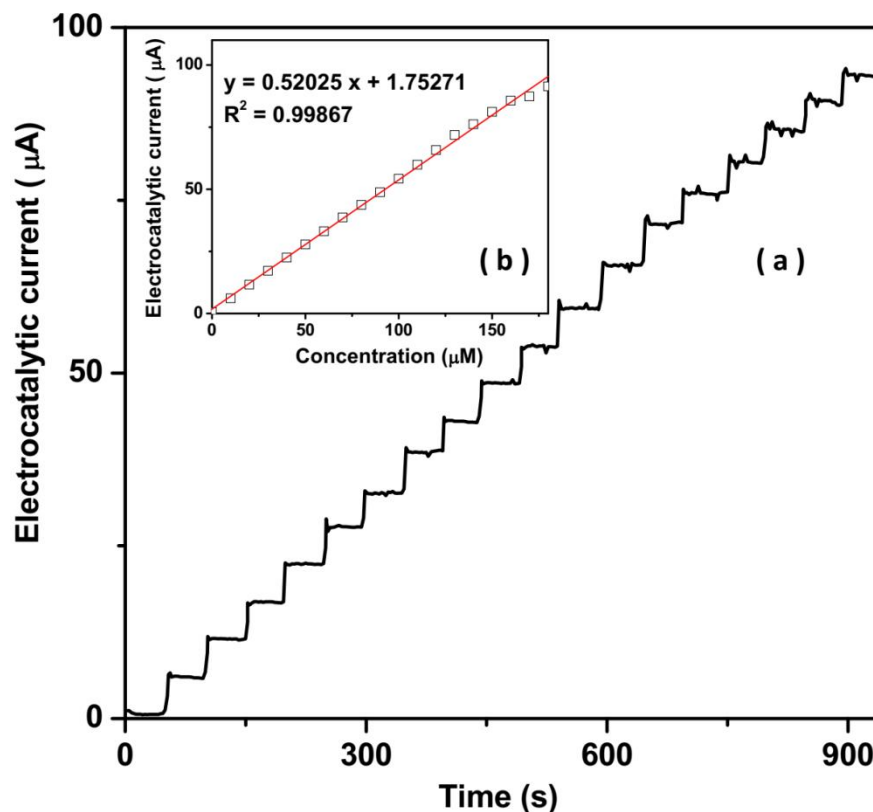


Figure 7. (a) The electrochemical amperometry response of cellulase/c-MWCNTs and (b) its calibration plot for successive addition of 10 μM catechol solution in 0.1 M PBS pH 4.0 containing 5 mM $[\text{Fe}(\text{CN})_6]^{3-/4-}$ at potential 0.11 V and temperature of 35°C.

Table 1. Comparison between the obtained detection limit and linear range values of catechol on cellulase/c-MWCNTs with other reported catechol sensor.

Modified electrode	Technique	Detection limit (μM)	Detection range (μM)	Ref.
MWNTs/GCE	DPV*	0.2	0.6 to 100	[43]
Graphene/GCE	DPV	0.01	1 to 50	[44]
Copper(II) complex/SWCNTs/GCE	DPV	3.5	5 to 215	[45]
Cu- mesoporous carbon/chitosan matrix	CV	0.67	0.6 to 15.7	[46]
Laccase/ ZnO/ chitosan/GCE	CV	0.290	1 to 100	[47]
Laccase/N doped mesoporous carbon/ polyvinyl alcohol matrix	amperometry	0.31	0.39 to 8.98	[48]
Hierarchical NiAl-layered double hydroxide	amperometry	0.003	0.01 to 400	[49]
Laccase /graphene-cellulase microfiber composite/ screen-printed carbon electrode	amperometry	0.085	0.2 to 209.7	[50]
Cellulase/c-MWCNTs	amperometry	0.004	10 to 160	This work

* DPV: Differential pulse voltammetry

The determination of catechol in extract solution of green tea sample was done in the electrochemical cell containing prepared 100 ml 0.1 M PBS (pH 4.0) containing 5 mM $[\text{Fe}(\text{CN})_6]^{3-/4-}$ of real sample using successive additions of the standard catechol solution. The amperogram was recorded after addition catechol solution at potential 0.11 V and temperature of 35°C. The cellulase/c-MWCNTs sensor was applied in prepared real sample and the obtained recovery and relative standard deviation (RSD) are shown in Table 2. As observed the range of recovery and RSD values resulted from 83.50% to 98.66% and 1.80% to 3.17%, respectively which indicated the developed sensor can be effectively used for catechol detection in real samples.

Table 2. Analytical results of catechol electrochemical determination in real samples using cellulase/c-MWCNTs (n = 4).

Real sample	Amount added ($\mu\text{g/l}$)	Found concentrations ($\mu\text{g/l}$)	Recovery (%)	Relative standard deviations (%)
green tea	2.00	1.87	93.50	2.11
	4.00	3.83	95.75	3.06
	6.00	5.92	98.66	1.80
	8.00	7.88	98.50	3.17

4. CONCLUSION

This work presented the enzymatic and electrochemical properties of cellulase immobilized on MWCNTs. The surface morphologies and attachment of impurities on the c-MWCNTs and cellulase/c-MWCNTs, enzyme activity and electrochemical properties were studied. Results of FESEM and FTIR showed that the c-MWCNTs were prepared in bundles with porous and smooth surfaces. The prepared cellulase/c-MWCNTs displayed the rougher surface with more saturated pores. These results confirmed the successful immobilization of cellulase enzyme on the c-MWCNTs side walls. The results of enzyme activity indicated that the optimum condition for electrochemical study of the cellulase/c-MWCNTs was obtained concentration of 4 mg/ml, pH 4 and temperature of 35°C. Electrochemical study of cellulase/c-MWCNTs for detection catechol showed linear range and detection limit were obtained 10 to 160 μM and 0.004 μM , respectively. The resulted sensing properties of cellulase/c-MWCNTs was compared with other reported catechol sensor which specified to the comparable electrochemical properties and low detection limit for determination of catechol on the cellulase/c-MWCNTs due to formation of fast electron transfer pathways between the cellulase/c-MWCNTs electrode and the electrolyte because of synergistic effect of porous morphology and nanometric cylindrical graphene sheets in the MWCNTs and cross linking and covalent bounds of cellulase.

ACKNOWLEDGEMENT

This work was sponsored in part by Seed Foundation of Jilin Agricultural Science and Technology University (20187003) and Research programs of the Education Department of Jilin Province, China (JJKH20190970KJ).

References

1. V. Juturu and J.C. Wu, *Renewable and Sustainable Energy Reviews*, 33 (2014) 188.
2. H. Karimi-Maleh, M. Alizadeh, Y. Orooji, F. Karimi, M. Baghayeri, J. Rouhi, S. Tajik, H. Beitollahi, S. Agarwal and V.K. Gupta, *Industrial & Engineering Chemistry Research*, 60 (2021) 816.
3. R. Mohamed, J. Rouhi, M.F. Malek and A.S. Ismail, *International Journal of Electrochemical Science*, 11 (2016) 2197.
4. B. Yuan, X.-q. Yang, L.-w. Xue, Y.-n. Feng and J.-h. Jiang, *Bioresource technology*, 222 (2016) 14.
5. J. Rouhi, S. Kakooei, M.C. Ismail, R. Karimzadeh and M.R. Mahmood, *International Journal of Electrochemical Science*, 12 (2017) 9933.
6. M. Bilal, M. Asgher, H. Cheng, Y. Yan and H.M. Iqbal, *Critical reviews in biotechnology*, 39 (2019) 202.
7. N.R. Mohamad, N.H.C. Marzuki, N.A. Buang, F. Huyop and R.A. Wahab, *Biotechnology & Biotechnological Equipment*, 29 (2015) 205.
8. J. Rouhi, S. Kakooei, S.M. Sadeghzadeh, O. Rouhi and R. Karimzadeh, *Journal of Solid State Electrochemistry*, 24 (2020) 1599.
9. S. Hirsh, M. Bilek, N. Nosworthy, A. Kondyurin, C. Dos Remedios and D. McKenzie, *Langmuir*, 26 (2010) 14380.
10. H. Karimi-Maleh, Y. Orooji, A. Ayati, S. Qanbari, B. Tanhaei, F. Karimi, M. Alizadeh, J. Rouhi, L. Fu and M. Sillanpää, *Journal of Molecular Liquids*, (2020) 115062.
11. B. Thangaraj and P.R. Solomon, *ChemBioEng Reviews*, 6 (2019) 157.
12. S. Changaei, J. Zamir-Anvari, N.-S. Heydari, S.G. Zamharir, M. Arshadi, B. Bahrami, J. Rouhi and R. Karimzadeh, *Journal of Electronic Materials*, 48 (2019) 6216.
13. N. Naderi, M. Hashim, J. Rouhi and H. Mahmodi, *Materials science in semiconductor processing*, 16 (2013) 542.
14. B. Jugović, B. Grgur, M. Antov, Z. Knežević Jugović, J.S. Stevanović and M.M. Gvozdenović, *International Journal of Electrochemical Science*, 11 (2016) 1152.
15. P. Gaikwad, D. Shirale, V. Gade, P. Savale, H. Kharat, K. Kakde and M. Shirsat, *International Journal of Electrochemical Science*, 1 (2006) 425.
16. A.A. Sehat, A.A. Khodadadi, F. Shemirani and Y. Mortazavi, *International Journal of Electrochemical Science*, 10 (2015) 272.
17. F. Colmati, S.A. Yoshioka, V. Silva, H. Varela and E.R. Gonzalez, *International Journal of Electrochemical Science*, 2 (2007)
18. H. Karimi-Maleh, S. Ranjbari, B. Tanhaei, A. Ayati, Y. Orooji, M. Alizadeh, F. Karimi, S. Salmanpour, J. Rouhi and M. Sillanpää, *Environmental Research*, 195 (2021) 110809.
19. S. Kakooei, J. Rouhi, E. Mohammadpour, M. Alimanesh and A. Dehzangi, *Caspian Journal of Applied Sciences Research*, 1 (2012) 16.
20. W. Zhang, J. Qiu, H. Feng, L. Zang and E. Sakai, *Journal of Magnetism and Magnetic Materials*, 375 (2015) 117.
21. D. Zhang, H.E. Hegab, Y. Lvov, L. Dale Snow and J. Palmer, *SpringerPlus*, 5 (2016) 48.
22. A. Negrulescu, V. Patrutea, M.M. Mincea, C. Ionascu, B.A. Vlad-Oros and V. Ostafe, *Journal of the Brazilian Chemical Society*, 23 (2012) 2176.
23. K.K. Kwon, S.-J. Yeom, D.-H. Lee, K.J. Jeong and S.-G. Lee, *Biochemical and biophysical research communications*, 495 (2018) 1328.

24. K. Luo, N.-g. Kim, S.-M. You and Y.-R. Kim, *Nanomaterials*, 9 (2019) 1291.
25. A.N. Chakoli, J. He, W. Cheng and Y. Huang, *RSC advances*, 4 (2014) 52372.
26. Y. Chen, K. Kang, K. Han, K. Yoo and J. Kim, *Synthetic Metals*, 159 (2009) 1701.
27. J. Sun, J. Xu, H. Jiang, X. Zhang and D.F. Niu, *ChemElectroChem*, 7 (2020) 1869.
28. B.P. Singh, V. Choudhary, S. Teotia, T.K. Gupta, V. Nand, S.R.D. Singh and R.B. Mathur, *Advanced Materials Letter*, 6 (2015) 104.
29. L.Y. Jun, N. Mubarak, L.S. Yon, C.H. Bing, M. Khalid, P. Jagadish and E. Abdullah, *Scientific reports*, 9 (2019) 1.
30. M.j. Velický, P.S. Toth, C.R. Woods, K.S. Novoselov and R.A. Dryfe, *The Journal of Physical Chemistry C*, 123 (2019) 11677.
31. A. Buchner, F. Tostevin, F. Hinzpeter and U. Gerland, *The Journal of chemical physics*, 139 (2013) 10B601.
32. S. Arana-Peña, N.S. Rios, D. Carballares, C. Mendez-Sanchez, Y. Lokha, L.R.B. Gonçalves and R. Fernandez-Lafuente, *Frontiers in bioengineering and biotechnology*, 8 (2020) 36.
33. Y.-W. Zhang, P. Prabhu and J.-K. Lee, *Bioscience, biotechnology, and biochemistry*, 73 (2009) 2234.
34. K. Vasić, Ž. Knez and M. Leitgeb, *Scientific Reports*, 10 (2020) 1.
35. J. Zhan, S. Jiang and L. Pan, *Brazilian Journal of Chemical Engineering*, 30 (2013) 721.
36. H.-X. Zhou and X. Pang, *Chemical reviews*, 118 (2018) 1691.
37. R. Chong-Cerda, L. Levin, R. Castro-Ríos, C.E. Hernández-Luna, A. González-Horta, G. Gutiérrez-Soto and A. Chávez-Montes, *Catalysts*, 10 (2020) 1085.
38. R.M. Daniel, M.J. Danson, R. Eiseenthal, C.K. Lee and M.E. Peterson, *Extremophiles*, 12 (2008) 51.
39. C. Kaçar, P.E. Erden and E. Kılıç, *Analytical and bioanalytical chemistry*, 409 (2017) 2873.
40. S. Soylemez, F.E. Kanik, S.D. Uzun, S.O. Hacıoglu and L. Toppare, *Journal of Materials Chemistry B*, 2 (2014) 511.
41. R. Savari, S. Soltanian, A. Noorbakhsh, A. Salimi, M. Najafi and P. Servati, *Sensors and Actuators B: Chemical*, 176 (2013) 335.
42. T.A. Freitas, A.B. Mattos, B.V. Silva and R.F. Dutra, *BioMed research international*, 2014 (2014) 1.
43. Y.-P. Ding, W.-L. Liu, Q.-S. Wu and X.-G. Wang, *Journal of Electroanalytical Chemistry*, 575 (2005) 275.
44. H. Du, J. Ye, J. Zhang, X. Huang and C. Yu, *Journal of Electroanalytical Chemistry*, 650 (2011) 209.
45. L.A. Alshahrani, X. Li, H. Luo, L. Yang, M. Wang, S. Yan, P. Liu, Y. Yang and Q. Li, *Sensors*, 14 (2014) 22274.
46. X. Xu, M. Guo, P. Lu and R. Wang, *Materials Science and Engineering: C*, 30 (2010) 722.
47. J. Qu, T. Lou, Y. Wang, Y. Dong and H. Xing, *Analytical Letters*, 48 (2015) 1842.
48. M. Guo, H. Wang, D. Huang, Z. Han, Q. Li, X. Wang and J. Chen, *Science and Technology of Advanced Materials*, 15 (2014) 035005.
49. M. Shen, Z. Zhang and Y. Ding, *Microchemical Journal*, 124 (2016) 209.
50. S. Palanisamy, S.K. Ramaraj, S.-M. Chen, T.C.K. Yang, P. Yi-Fan, T.-W. Chen, V. Velusamy and S. Selvam, *Scientific Reports*, 7 (2017) 41214.